

ESTIMATION OF THE ACCURACY OF LASER GUIDED BOMB

Grzegorz Kowaleczko, Mariusz Pietraszek

*Air Force Institute of Technology
Ksiecia Boleslawa 6, 01-494 Warsaw, Poland
tel.: +48 261851300
e-mail: g.kowaleczko@chello.pl*

Abstract

The main goal of the bomb release is to hit the target with a maximum accuracy. Therefore, special active control systems are utilized to improve this accuracy. Some of the most popular are semi-active laser systems of guidance. Selected target is pointed with high-intensity laser by an airborne or ground laser designator. The laser-guided bomb (LGB) tracks this target using on-board laser seeker and adjusts its trajectory.

The main task of the control system is to steer the bomb in the way allowing fixing the reflected laser beam in the centre of photo sensor array. This keeps the bomb axis straight toward the target.

The aim of this study is to identify factors influencing on the accuracy of the LGB. It was performed for the prototype of LGB, which was designed in the Air Force Institute of Technology. This is the modernized version of the classical LB-10M bomb. Originally, this bomb has only four rear stabilizers and it has been equipped with four additional fins (Fig. 1). These fins allow controlling the bomb's path in active way. Earlier studies have shown that this is the useful method of bomb control both in longitudinal and lateral motions. Analysis proved that range of the bomb can be effectively changed.

This paper presents method of flight simulations for released LGB. Calculations were performed using six-degrees-of-freedom mathematical model of the LB-10M bomb motion. Aerodynamics was calculated using commercial software. Control laws were determined based on signals detected by two pairs of laser sensors. Exemplary results of simulations are submitted and conclusions focused on the main factors influencing on bombing accuracy are shown.

Keywords: *exterior ballistics, guided munitions, flight control*

1. Introduction

The main goal of the bomb release is to hit the target with a maximum possible degree of accuracy. Therefore, special active control systems are utilised to improve this accuracy. Some of the most popular are semi-active laser systems of guidance. Selected target is pointed and illuminated with high-intensity laser (usually in infrared spectrum) by an airborne or ground laser designator (separate humans' operator, either in the air or on the ground). The laser-guided bomb (LGB) tracks this target using on board laser seeker (an array of photo diodes) and adjusts its trajectory. Therefore, the LGB is a manoeuvrable, freefall weapon that guides to a spot of laser energy reflected off the target. The LGB is delivered like a normal general-purpose warhead, and the semi active guidance corrects many of the normal errors inherent in any delivery system.

The main task of the control system is to steer the bomb in the way allowing fixing the reflected laser beam in the centre of photo sensor array. This keeps the bomb axis straight toward the target. LGB's are active until after release and require no modifications or electrical interface with the delivery aircraft.

First laser-guided bomb were operationally used in Vietnam War in 1968 and next in the operation Desert Storm in 1991. Data from these wars show that the accuracy of the LGB's is significantly higher than for unguided bombs (50% for LGB versus 5.5% for unguided bombs). Allowing to their precision, laser guided bombs can be less explosive and they cause less collateral damage than unguided bombs.

Nowadays one can find many various types of LGB. They are one of the most widespread guided munitions, used by many of the world's air forces. All LGBs consist of a laser guidance kit attached to the nose and a tail of standard general-purpose warhead. The laser guidance kit is composed of two major components that are attached to the warhead – a common computer control group (CCG) that attaches to the nose of all warheads and a warhead specific airfoil group (AFG). AFG consists of a tail-mounted wing assembly and properly sized control fins that match the common CCG to the aerodynamics of the variety of warheads adapted for LGB use. The control fins are composed of two pairs of small wings (fins), which can be moved up down or left-right to change trajectory of the LGB - they provide some extra lift to manoeuvre.

The aim of this study is to identify crucial factors influencing on the accuracy of the LGB. It was performed for the prototype of Polish LGB, which was designed in the Air Force Institute of Technology. This is modernized version of the LB-10M bomb designed in 2008. Originally, this bomb has only four rear stabilizers (Fig. 1) and it has been equipped with four additional fins (Fig. 2). These fins allow controlling the bomb's path in active way. It was proved in [6] that this is the useful method of bomb control both in longitudinal and lateral motions. Analysis showed that range of the bomb can be effectively changed.

Determination of control laws and identification of main factors influencing on LGB accuracy are the next steps of works devoted to the modernized LB-10M bomb. They are still under investigations. Preliminary results are presented in this paper. They are obtained using numerical simulations of spatial controlled flight of the bomb.



Fig. 1. LB-10M bomb mounted on TS-11 plane



Fig. 2. LB-10M bomb with additional fins and laser seeker

2. Mathematical model of bomb's motion

Mathematical model of the bomb motion is based on assumptions that the bomb is a rigid body and it has two planes of symmetry. This model has been presented in details in [5, 6]. Similar descriptions of projectile motion can be found in [1-4, 7].

Therefore, we show only the final equations:

Tab. 1. Motion equations

$m(\dot{U} + QW - RV) = X$	$m(\dot{V} + RU - PW) = Y$	$m(\dot{W} + PV - QU) = Z$
$I_x \dot{P} = L$	$I_y \dot{Q} - (I_z - I_x)RP = M$	$I_z \dot{R} - (I_x - I_y)PQ = N$
$\dot{\Psi} = (R \cos \Phi + Q \sin \Phi) / \cos \Theta$	$\dot{\Theta} = Q \cos \Phi - R \sin \Phi$	$\dot{\Phi} = P + (Q \sin \Phi + R \cos \Phi) \tan \Theta$
$\begin{bmatrix} \dot{x}_g \\ \dot{y}_g \\ \dot{z}_g \end{bmatrix} = \mathbf{L}_{g/b} \begin{bmatrix} U \\ V \\ W \end{bmatrix}$	$\mathbf{L}_{g/b} = \begin{bmatrix} \cos \Psi \cos \Theta & \cos \Psi \sin \Theta \sin \Phi - \sin \Psi \cos \Phi & \cos \Psi \sin \Theta \cos \Phi + \sin \Psi \sin \Phi \\ \sin \Psi \cos \Theta & \sin \Psi \sin \Theta \sin \Phi + \cos \Psi \cos \Phi & \sin \Psi \sin \Theta \cos \Phi - \cos \Psi \sin \Phi \\ -\sin \Theta & \cos \Theta \sin \Phi & \cos \Theta \cos \Phi \end{bmatrix}$	

where: m – mass of the bomb; I_x, I_y, I_z – inertia moments, U, V, W – components of the velocity vector; P, Q, R – rolling, pitching and yawing angular velocities; X, Y, Z – components of the sum of the weight and aerodynamic force; L, M, N – roll, pitch and yaw aerodynamic moments. Forces and moments were calculated from formulas:

Tab. 2. Forces and moments

Forces: $X = X_g + X_{aer}$, $Y = Y_g + Y_{aer} + F_{y_control}$ $Z = Z_g + Z_{aer} + F_{z_control}$		
$X_g = -mg \sin \Theta$	$X_{aer} = -C_x \frac{\rho V_{aer}^2}{2}$	$V_{aer} = \sqrt{U^2 + V^2 + W^2}$
$Y_g = mg \cos \Theta \sin \Phi$	$Y_{aer} = \frac{\rho V_{aer}^2}{2} S \cdot \left[C_{N\delta} \left(\frac{-V}{V_{aer}} \right) + \left(\frac{Rd}{V_{aer}} \right) C_{Nq} \right]$	$F_{y_control} = \frac{\rho V_{aer}^2}{2} S \cdot C_{N_F2}^\delta \delta_N$
$Z_g = mg \cos \Theta \cos \Phi$	$Z_{aer} = -\frac{\rho V_{aer}^2}{2} S \cdot \left[C_{N\delta} \left(\frac{-W}{V_{aer}} \right) + \left(\frac{-Qd}{V_{aer}} \right) C_{Nq} \right]$	$F_{z_control} = -\frac{\rho V_{aer}^2}{2} S \cdot C_{N_F2}^\delta \delta_M$
Moments: $L = L_{aer}$, $M = M_{aer} + M_{control}$ $N = N_{aer} + N_{control}$		
$L = \frac{\rho V_{aer}^2}{2} S d C_{lp} \left(\frac{Pd}{V_{aer}} \right)$		
$M = \frac{\rho V_{aer}^2}{2} S d \cdot \left[C_{m\delta} \left(\frac{W}{V_{aer}} \right) + C_{mq} \left(\frac{Qd}{V_{aer}} \right) \right]$	$M_{control} = -l_{F2} \cdot F_{z_control}$	
$N = \frac{\rho V_{aer}^2}{2} S d \cdot \left[C_{n\delta} \left(\frac{-V}{V_{aer}} \right) + C_{nq} \left(\frac{Rd}{V_{aer}} \right) \right]$	$N_{control} = l_{F2} \cdot F_{y_control}$	

where: $C_x, C_{N\delta}, C_{Nq}$ – coefficients of aerodynamic axial and normal forces, $C_{lp}, C_{m\delta}, C_{mq}, C_{n\delta}, C_{nq}$ – coefficients of aerodynamic moments, S – cross-sectional area of the bomb, ρ – air density, d – diameter of the bomb, l_{F2} – the distance between the pressure centre of fins and the centre of mass. δ_M, δ_N – deflections of two pairs of fins in lateral and longitudinal motions. Because of bomb's symmetry one has: $C_{n\delta} = C_{m\delta}, C_{nq} = C_{mq}$. All aerodynamic coefficients were determined using commercial software *Prodas*. They are presented in [6].

3. Seeker characteristics

Geometry

Determination of the geometry of the seeker detectors with respect to both the bomb and to the target is necessary to calculate control laws. In the case of investigated LB-10M bomb, the seeker detectors are mounted as it is shown in Fig. 2-4. Geometry of detectors is defined by their coordinates in $Oxyz$ system fixed with the bomb and by the angle ϕ_{det} ; (Fig. 3). This angle allows calculating unit vector \mathbf{w}_{det} of each detector (Fig. 4). They are presented in the table below:

Tab. 3 Coordinates and unit vector of detectors

Detector	Coordinates	Unit vector
upper	$\mathbf{r}_u = [l_{det}, 0, -h_{det}]$	$\mathbf{w}_u = [\cos \phi_{det}, 0, -\sin \phi_{det}]^T$
lower	$\mathbf{r}_d = [l_{det}, 0, h_{det}]$	$\mathbf{w}_d = [\cos \phi_{det}, 0, \sin \phi_{det}]^T$
right	$\mathbf{r}_r = [l_{det}, h_{det}, 0]$	$\mathbf{w}_r = [\cos \phi_{det}, \sin \phi_{det}, 0]^T$
left	$\mathbf{r}_l = [l_{det}, -h_{det}, 0]$	$\mathbf{w}_l = [\cos \phi_{det}, -\sin \phi_{det}, 0]^T$

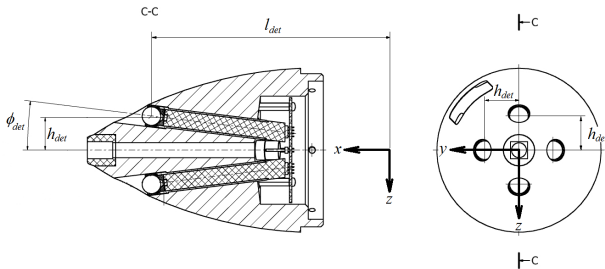


Fig. 3. Geometry of detectors

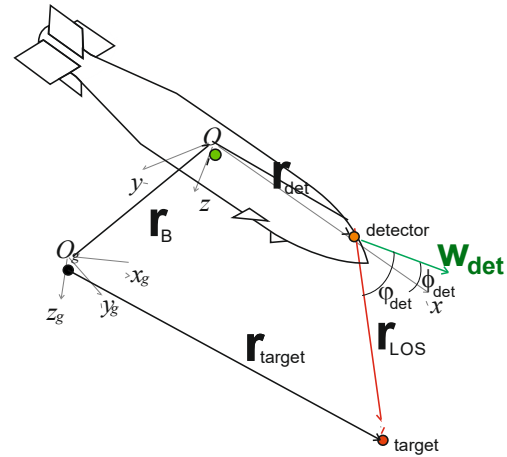


Fig. 4. Detector-bomb-target geometry

The line-of-sight (LOS) for the detector is a line connecting the detector with the target. Figure 4 schematically shows \mathbf{r}_{LOS} vector corresponding to the LOS and other vectors used to calculate \mathbf{r}_{LOS} :

- vector of the bomb position defined in the system $O_g x_g y_g z_g$, $\mathbf{r}_B = [x_{g_b}, y_{g_b}, z_{g_b}]^T$,
- vector of the target position defined in the system $O_g x_g y_g z_g$, $\mathbf{r}_{target} = [x_{g_target}, y_{g_target}, z_{g_target}]^T$,
- vector of the detector position defined in the system $Oxyz$, $\mathbf{r}_{det} = [x_{det}, y_{det}, z_{det}]^T$ – see Tab. 3.

To determine LOS it must know the positions of the target and detector in the same coordinate system. This means that all vectors should be specified in the same frame. The analysis assumes that this is the $Oxyz$ system fixed with the bomb. The Figure 4 indicates that:

$$\mathbf{r}_B + \mathbf{r}_{\text{det}} + \mathbf{r}_{\text{LOS}} - \mathbf{r}_{\text{target}} = \mathbf{0}. \quad (1)$$

Using the transformation matrix $\mathbf{L}_{g/b}$ from the system $O_gx_gy_gz_g$ to $Oxyz$, one can obtain relationship, which allows calculating the coordinates of \mathbf{r}_{LOS} vector in the system $Oxyz$:

$$\begin{bmatrix} x_{\text{LOS}} \\ y_{\text{LOS}} \\ z_{\text{LOS}} \end{bmatrix} = \mathbf{L}_{g/b}^{-1} \left(\begin{bmatrix} x_{g_targ} \\ y_{g_targ} \\ z_{g_targ} \end{bmatrix} - \begin{bmatrix} x_{g_b} \\ y_{g_b} \\ z_{g_b} \end{bmatrix} \right) - \begin{bmatrix} x_{\text{det}} \\ y_{\text{det}} \\ z_{\text{det}} \end{bmatrix}. \quad (2)$$

To determine the angle φ_{det} between the vector \mathbf{r}_{LOS} and the detector unit vector \mathbf{w} /subscripts omitted/ one can use the following relationship:

$$\varphi_{\text{det}} = \arccos \frac{\mathbf{r}_{\text{LOS}} \circ \mathbf{w}}{|\mathbf{r}_{\text{LOS}}| \cdot |\mathbf{w}|} = \arccos \frac{x_{\text{LOS}}x_w + y_{\text{LOS}}y_w + z_{\text{LOS}}z_w}{\sqrt{x_{\text{LOS}}^2 + y_{\text{LOS}}^2 + z_{\text{LOS}}^2}}, \quad (3)$$

wherein the components of vector \mathbf{r}_{LOS} are determined from equation (2) and components of the vector \mathbf{w} are defined in Tab. 3. The relation $|\mathbf{w}| = 1$ is taken into account in (3).

Shown above calculations should be performed for each of detectors.

Sensitivity of detectors

It is assumed that energy of the signal detected by the single i -th sensor depends on the angle φ_{det} between the line-of-sight and the longitudinal axis of the detector. The power of detected signal influences on the voltage generated by the detector. Figure 5 shows theoretical, normalized characteristics of a single detector. The presented characteristics are defined by the formula:

$$\frac{G_i(\varphi_i)}{G_0} = e^{-\frac{1}{2} \left(\frac{\varphi_i}{\sigma} \right)^2}, \quad (4)$$

where:

G_0 – maximum voltage generated by the detector,

σ – standard deviation.

Note that signals G_i have always-positive sign. This corresponds to the real conditions of detection - a detected signal does not contain information about LOS direction, but only about its deviation with respect to the axis of the detector.

It is assumed that all detectors have the same characteristics. In the future simulations it will be replaced by the characteristics obtained from the results of measurements.

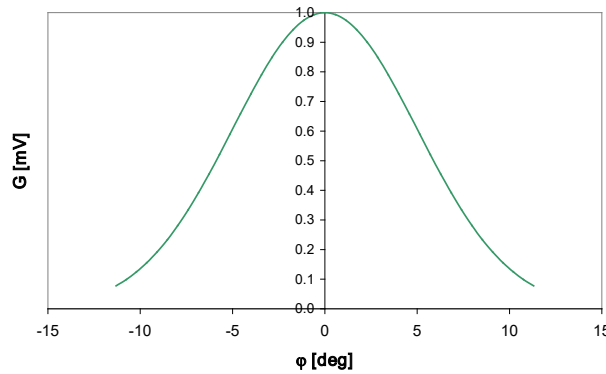


Fig. 5. Normalized detector characteristics ($G_0=1$)

4. Control laws

One of the most important parts of the LGB is a computer of the CCG, which contains circuitry that processes electrical signals from the detector and develops the directional command signals for the control fins. In studies of the guided bombs, there is no detailed information about applied control laws. Therefore, in this work it is assumed that the control signals are proportional to differences between signals detected by pairs of sensors located in the same plane, i.e.: up-down and left-right:

– in the plane Oxz (up-down):

$$\delta_M = k_\Delta \Delta G_{ud} = k_\Delta (G_u - G_d), \quad (5)$$

– in the plane Oxy (left-right):

$$\delta_N = k_\Delta \Delta G_{lr} = k_\Delta (G_l - G_r), \quad (6)$$

k_Δ is the control law coefficient. Additionally, the limitation $\pm 10^\circ$ for fins deflections are taken into account.

5. Results of simulations

Simulations were performed assuming that the bomb is released by an aircraft performing steady state horizontal flight, for the following initial conditions: the altitude – 3000 meters, the velocity – 55.56 m/s (200/km/h), the pitch angle 0° . The target is located 1600 meter in front of the point of release.

At the beginning, the unguided bomb was tested (Fig. 6÷9). Calculations show that the bomb falls after time of 25.706 seconds at the distance of 1311 meters. The final velocity is equal to 221.2 m/s. The LOS angle φ_{det} (absolute value) of the lower detector decreases, next for 13.49 sec is equal to zero (detector coincidences with LOS) and finally φ_{det} starts to increase – Fig. 9.

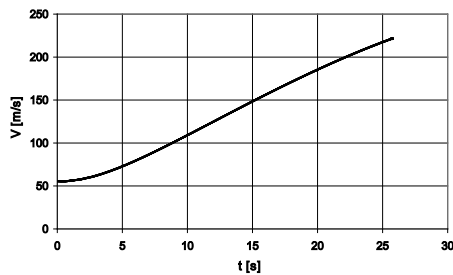


Fig. 6. Bomb velocity

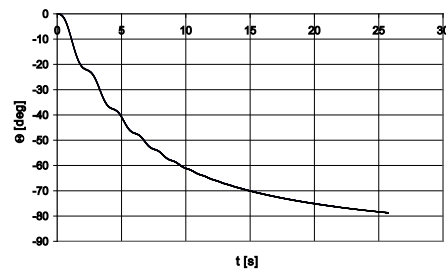


Fig. 7. Pitch angle

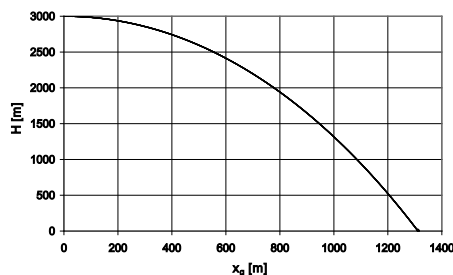


Fig. 8. Vertical trajectory

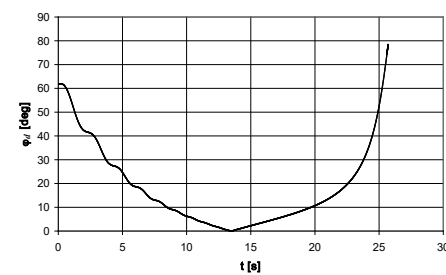


Fig. 9. LOS angle

Next, a flat drop in vertical plane was tested for various values of the coefficient k_Δ . Because the target is in the plane Oxz that the right and left sensors give the same signal ($G_r = G_l$) and the control angle δ_N is equal to zero. The signals G_u and G_d are calculated based on the formula (5) for values: (a) - $k_\Delta = 5 \cdot 10^2$, (b) - $k_\Delta = 1 \cdot 10^3$, (c) - $k_\Delta = 2 \cdot 10^3$. Results are shown in figures 10-16. It can

be seen (Fig. 10) that in any case the bomb does not reach the target – the reached range is equal to: (a) – 1543 m, (b) – 1565 m, (c) – 1572 m. This is due to the fact that the trajectory pitch angle is greater than the bomb pitch angle. Therefore, even if the LOS coincides with the axis of the bomb, the flight path is directed to a point located before the target. This is shown in Figure 11.

The increase of the coefficient k_{Δ} improves accuracy, but to a limited range. At the same time, this increase generates growing oscillations of the flight parameters. This is visible in Figures 12 and 13 showing the angle of attack and the pitch angle. The consequences of this are, in turn, oscillations of the angle of LOS, as shown in Figure 14 for the lower detector and oscillations of the signal generated by this detector (Figure 15). These last two figures prove that the most precise guidance during the second phase of the flight was obtained in the (c) case. Figure 16 shows the control angle δ_M . It confirms that the increase of k_{Δ} values significantly increases the oscillation of the control angle δ_M .

It should be noted that in the final phase of flight, in each case, the control angle reaches a maximum value. This is due to the fact that the divergence between the trajectory and the LOS is strongly increased. Based on the above analysis, for further calculations, the value corresponding to the case (b), i.e. $k_{\Delta}=1*10^3$ was taken into account.

As it was previously noted, the range of the unguided bomb is 1311 meters. Other calculations were performed for the target location in the range of 1000÷2050 meters. The longitudinal error – the distance between the hit point and the target – is shown in Figure 17. One can see that this error increases for increasing location of the target.

Next simulations were done for the case of asymmetric location of the target. Calculations were carried out for $k_{\Delta}=1*10^3$, assuming the constant coordinate value $x_{g_targ}=1600$ meters and y_{g_targ} in the range 0÷500 meters. In this case, control of the bomb is effective, but the lateral error is also observed. This is shown in Fig. 18. Figure 19 presents the control angle δ_N for y_{g_targ} : (a) - 50 m, (b) - 250 m, (c) - 500 m. One can see that this angle varies depending on the variant of calculations and it can reach the limit $\pm 10^0$.

Presented above results were done for the "+" initial configuration of the bomb. Because the "x" configuration is also possible and often exploited, this configuration was also tested. Figures 20 and 21 show control angles for asymmetric target location: $x_{g_targ}=1600$ meters and $y_{g_targ}=250$ meters. Other results obtained for the "x" configuration show that the target is reached but also with limited accuracy.

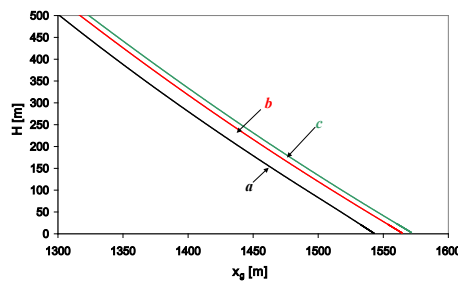


Fig. 10. Final vertical trajectory

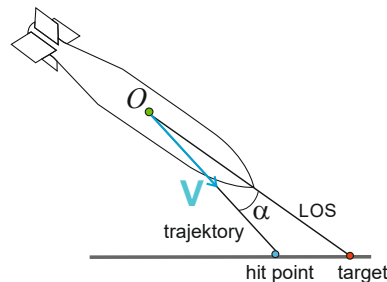


Fig. 11. Final configuration of the bomb

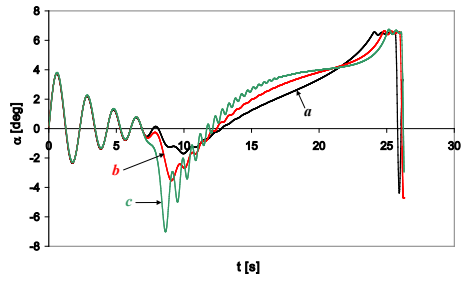


Fig. 12. Angle of attack

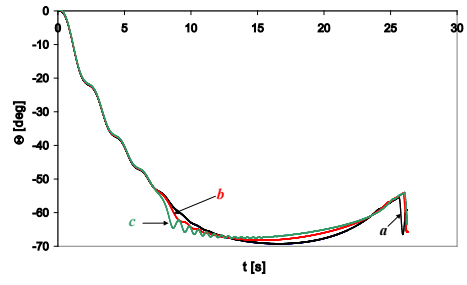


Fig. 13. Pitch angle

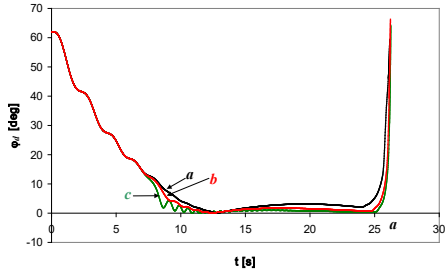


Fig. 14. LOS angle

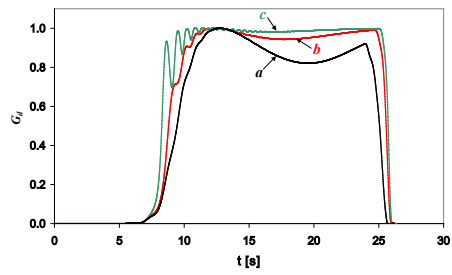


Fig. 15. Lower detector signal G_d

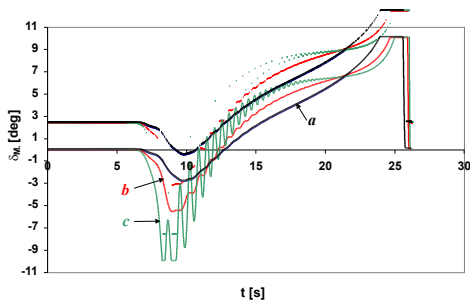


Fig. 16. Control angle δ_M

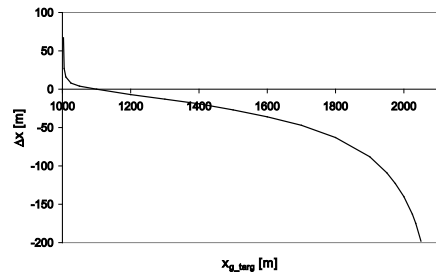


Fig. 17. Longitudinal error

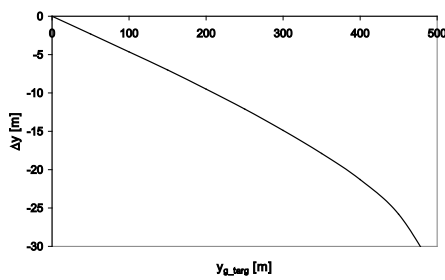


Fig. 18. Lateral error

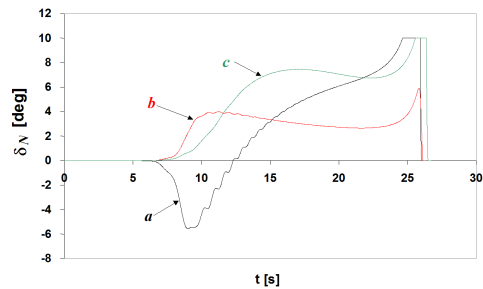


Fig. 19. Control angle δ_N

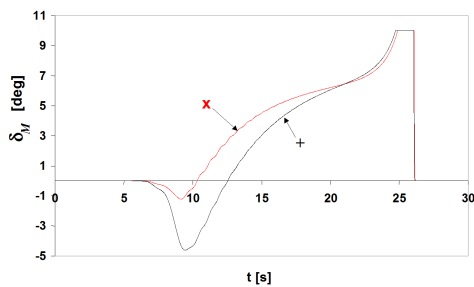


Fig. 20. Control angle δ_M for two bomb configurations

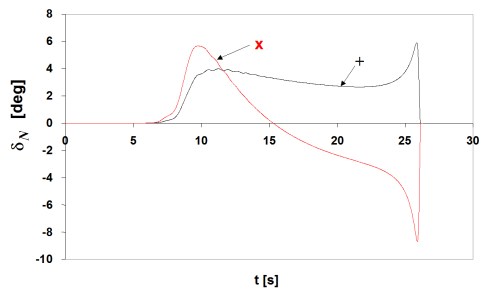


Fig. 21. Control angle δ_N for two bomb configurations

6. Conclusions

The conducted analysis has proved that the laser-guided bomb may be efficiently controlled by laser seeker but its accuracy is limited for applied control laws and for used initial conditions. It means that the further works have to be focused on modification of control laws. Different initial values of the release altitude, velocity and angle of release have to be also checked.

References

- [1] Carlucci, D. E., Jacobson, S. S., *Ballistics – Theory and Design of Guns and Ammunitions*, CRC Press, 2007.
- [2] Dimitriewskij, A. A., *External Ballistics*, Mashinostrojenie, Moscow 1972 (in Russian).
- [3] *Engineering Design Handbook – Design for Control of Projectile Flight Characteristics*, Headquarters U.S. Army Materiel Command, September 1996.
- [4] Gacek, J., *External Ballistics*, MUT, Warsaw 1999.
- [5] Kowaleczko, G., Żyluk, A., *Influence of atmospheric turbulence on bomb release*, Journal of Theoretical and Applied Mechanics, No. 1, Vol. 47, 2009.
- [6] Kowaleczko, G., Olejniczak, E., Pietraszek, M., Żyluk, A., *Evaluation of the Possibility of Bomb Flight Control*, Journal of KONES, 2015.
- [7] McCoy, R. L., *Modern Exterior Ballistics*, Schiffer Publishing Ltd., 2012.

